

Triplet Probe Study of the Excluded Volume Effect on the Rates of Diffusion-Controlled Intermacromolecular Reactions between Chain End Groups of Polystyrene

Kazuyuki Horie* and Itaru Mita

Institute of Space and Aeronautical Science, University of Tokyo, Komaba, Meguro-ku, Tokyo 153, Japan. Received May 8, 1978

ABSTRACT: The effects of molecular weight and solvent on the rate constants k_q for quenching of phosphorescence of polystyrylbenzil by polystyrylanthracene (model reaction for diffusion-controlled termination process in radical polymerization) have been studied in benzene, cyclohexane, and butanone at 20–40 °C by using a 10-ns dye laser or a nitrogen laser pulse. The k_q in benzene is inversely proportional to the 0.29 power of the degree of polymerization P for the range of $P = 23$ –3900. The reduced rate constants $k_q\eta_0/T$ in poor solvents are larger than $k_q\eta_0/T$ in good solvent for $P < 10^3$ and are opposite for $P > 10^3$. The results for lower P agree well with the prediction by previously proposed models including the thermodynamic (equilibrium) excluded volume effect. The results for higher P together with the inversion of solvent dependence of the reactivity require the concept of kinetic (nonequilibrium) excluded volume effect caused by topological hindrance of polymer chains for the encounter of active sites.

The mechanism of diffusion-controlled macromolecular reactions has become an attractive subject in recent years. In the previous paper¹ we reported for the first time direct measurements with a triplet probe for diffusion-controlled rate constants of polymer–polymer reactions between two chain ends of monodisperse macromolecules. The effect of molecular weight on rate constants has been shown there.

The effect of solvent on reaction rates will be another important factor to be considered. Solvent is supposed to affect the rates of diffusion-controlled polymer–polymer reactions not only through the change in its viscosity but also through the change in its interaction parameter with polymer chains. The latter is the cause of the excluded volume effect which has been one of the main subjects in investigations of solution properties of polymers for long years.

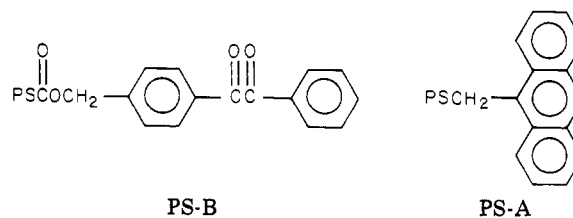
Conflicting conclusions have been presented so far concerning excluded volume effect on the diffusion-controlled rates of polymer–polymer reactions. The present authors² and Ito³ as well as Mahabadi and O'Driscoll⁴ have supposed that the rate constant k for diffusion-controlled polymer–polymer reactions in good solvent should be smaller than k in poor solvent, since the interpenetration of two polymer spheres would be smaller in good solvent than in poor solvent due to the increasing Flory's repulsive potential of average force. On the other hand, Cameron et al.⁵ and Schnabel et al.^{6,7} have measured k for reactions between two polymer molecules with different coil expansions and reported the k in poor solvent to be smaller than k in good solvent probably due to the formation of tightly coiled macromolecules which hinder the reaction between active sites. Morawetz et al. have proposed a model⁸ for the excluded volume effect on the rates of activation-controlled reaction between two polymer reagents which results in k in good solvent being smaller than k in poor solvent, while their experimental results⁹ conflict with their supposition from the model. This situation mentioned above forced us to elucidate the excluded volume effect on polymer–polymer reactions experimentally by measuring molecular weight and solvent dependences of the rates between monodisperse polymers with a definite active site on each molecule.

In the previous work,¹ quenching rates of phosphorescence of the benzil group attached to a chain end of polystyrene by the anthryl group attached to a chain end of another polystyrene have been measured in benzene

for the range of degree of polymerization $P = 23$ –740. In the present paper, the measurements of the quenching rates are extended to the reactions in poor solvents, i.e., in cyclohexane and in butanone, and also to a higher degree of polymerization ($P = 23$ –3900) by using a 10-ns dye laser and nitrogen laser pulses. Comparison of the results with our previously proposed model² and discussion resolving the confliction will be given about the excluded volume effect on diffusion-controlled polymer–polymer reactions.

Measurements of Quenching Rate Constants

Benzil or anthracene was attached to the chain end of anionically prepared polystyrene in the same procedure as previously reported.¹ The structure of polystyrene having the benzil or anthryl group at the chain end (PS-B or PS-A, respectively) is shown below.



Molecular weights and molecular weight distributions of PS-B and PS-A measured with a gel permeation chromatograph (GPC) as well as the content of anthryl group at the chain end of PS-A measured with an ultraviolet spectrophotometer are shown in Table I. The content of the benzil group at the chain end in several PS-B was determined to be about 80% from visible absorption spectra of PS-B. Dotite-Luminasol grade benzene and cyclohexane as well as Dotite-Spectrosol grade butanone were used as solvents for phosphorescence measurements.

The bimolecular rate constant of phosphorescence quenching k_q was calculated by using

$$1/\tau = 1/\tau_0 + k_q[A] \quad (1)$$

where τ and τ_0 are triplet lifetimes of phosphorophore in the presence and absence of quencher, respectively, and $[A]$ is the concentration of the anthryl group. The lifetimes τ and τ_0 were obtained from decay curves of phosphorescence intensity induced by a laser pulse with a half-width of 10 ns.

In cases where the concentration of benzil group $[B]$ is larger than 10^{-4} M, degassed sample solution was excited by a dye laser pulse of 406 nm where no absorption by

Table I
Characterization of PS-B and PS-A

polymer	\bar{M}_n	\bar{M}_w/\bar{M}_n	P of poly-styrene moiety	% anthryl group at a chain end
PS23-B	2.54×10^3	1.02	23	100
PS25-A	2.84×10^3	1.03	25	
PS60-B	6.40×10^3	1.10	60	
PS71-A	7.54×10^3	1.13	71	95.9
PS210-B	2.19×10^4	1.06	208	89.7
PS270-A	2.85×10^4	1.17	270	
PS660-B	6.84×10^4	1.08	660	
PS740-A	7.74×10^4	1.14	740	60.9
PS2600-B	2.73×10^5	1.13	2620	72.7
PS3300-A	3.45×10^5	1.23	3320	
PS2900-B	2.99×10^5	1.10	2870	
PS3900-A	4.11×10^5	1.34	3940	44.0

anthryl group was observed. The apparatus and procedure for measurements were the same as previously reported.¹ In order to prepare dilute solutions of PS-B and PS-A with P larger than 6×10^2 , the concentration of benzil group [B] should be less than 10^{-4} M. In cases where [B] $< 10^{-4}$ M, the sample solution was excited directly by a nitrogen laser pulse of 337 nm having much larger power than the pulse from dye laser. The application of 337-nm pulse instead of 406-nm pulse brings about two points to be checked: the first is about the presence of emission of PS-A, the second is about the change in [A] due to the excitation of PS-A. The overlap of fluorescence or delayed fluorescence emission from PS-A ($\lambda_{\max} = 420$ nm) on phosphorescence decay curves ($\lambda_{\max} = 560$ nm) could not be ignored for solutions of PS-B and PS-A with $P > 2 \times 10^3$, in spite of the uses of cutoff filters for $\lambda < 530$ nm and a cutoff gate circuit operating for 100 ns after pulse irradiation. So for these cases corrections were made by using blank decay curves for corresponding PS-A solutions without PS-B, as shown in Figure 1. The concentration of the excited triplet state anthryl group during the measurement in the microsecond region was calculated to be less than 3% of [A] when excited by the nitrogen laser. Since this amount was within the range of error of the

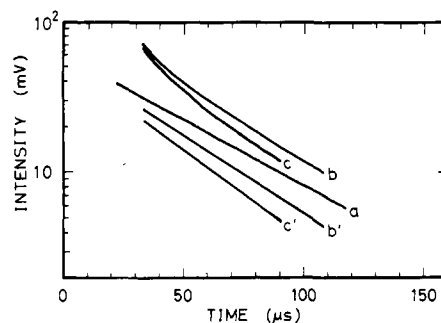


Figure 1. Uncorrected (a, b, c) and corrected (b', c') semilogarithmic decay curves for quenching of PS2600-B by PS3300-A in benzene at 30 °C. Concentrations: (a) [B] = 3.7×10^{-5} M; (b, b') [B] = 1.8×10^{-5} M, [A] = 0.75×10^{-5} M; (c, c') [B] = 1.6×10^{-5} M, [A] = 1.07×10^{-5} M.

present experiments, the values of [A] were uncorrected in the calculation of k_q .

In order to show the reproducibility for rate constants k_q and the applicability of the 337-nm pulse, the conditions and results for several experimental runs are listed in Table II. The applicability of the 337-nm pulse from the nitrogen laser instead of the 406-nm pulse from the dye laser was ascertained by measurements for solutions of PS210-B and PS270-A in benzene. Both experiments with 406-nm pulse and with 337-nm pulse gave the same rate constant k_q within the range of error. The percentages of error were about 5% for polymer with $P < 10^2$ and about 10% for $P > 10^2$ in most cases. They happened to reach about 20% in a few cases as are seen in Table II. All experiments except for the solution of PS660-B and PS740-A in cyclohexane with the 406-nm pulse were carried out under the condition of dilute solution (polymer concentration was lower than 10 g/dm³), where polymer molecules were supposed to be located separately in equilibrium.¹⁰ The results for the semidilute solution of PS660-B and PS740-A in cyclohexane and in benzene,¹ however, were consistent with the others measured in dilute solution. The solubility of PS-B and PS-A in cyclohexane decreases with decreasing temperature (Θ condition at 34.4 °C)¹¹ and with

Table II
Typical Experimental Conditions and Results for Polymer-Polymer Reactions

phosphorophore	[B] $\times 10^5$, M	quencher	[A] $\times 10^5$, M	solvent	polymer concn, g/dm ³	excitation wave-length, nm	$(1/\tau) \times 10^{-4}$, (40 °C), s ⁻¹	$k_q \times 10^{-9}$, (40 °C), M ⁻¹ s ⁻¹
PS210-B	12	PS270-A	0.71	benzene	2.7	406	3.57	0.832
	10				2.4		4.16	
	11				2.9		4.47	
PS210-B	12	PS270-A	0.71	benzene	2.7	337	3.29	0.752
	10				2.4		3.82	
	11				2.9		4.41	
PS2600-B	3.7	PS3300-A	0.75	benzene	9.9	337	2.85	0.380
	1.8				8.5		3.14	
	1.6				9.4		3.15	
PS2900-B	0.9	PS3900-A	0.50	benzene	2.7	337	2.02	0.358
	1.0				7.5		2.20	
	1.0				9.2		2.29	
PS660-B	46	PS740-A	3.11	cyclohexane	32	406	4.09	0.378
	46				35		5.27	
	51				43		6.39	
PS660-B	3.4	PS740-A	0.61	cyclohexane	2.3	337	0.785	0.380
	4.3				4.1		1.02	
	4.9				5.8		1.79	
PS2600-B	1.8	PS3300-A	0.71	cyclohexane	4.9	337	1.51	0.139
	1.8				8.2		1.61	
	1.7				9.9		1.70	
PS660-B	3.5	PS740-A	0.92	butanone	2.4	337	1.14	0.909
	3.9				3.8		1.98	
	5.6				6.5		2.94	

Table III
Quenching Rate Constants k_q and Their Activation
Energies E_q in Various Solvents

phospho- ro-phore	quencher	solvent	$k_q \times 10^{-9}, \text{M}^{-1} \text{s}^{-1}$			E_q , kJ/mol
			20 °C	30 °C	40 °C	
PS210-B	PS270-A	benzene	0.61	0.72	0.75	8.9
PS2600-B	PS3300-A		0.22	0.33	0.33	12.7
PS2900-B	PS3900-A		0.26	0.33	0.37	11.3
Benzil	anthra- cene	cyclo- hexane	3.9	4.1	4.9	12.0
Benzil	9-methyl- anthra- cene	hexane	2.8	3.4	4.0	12.8
PS23-B	PS25-A		1.0	1.2	1.3	10.8
PS60-B	PS71-A		0.82	0.96	1.1	10.7
PS210-B	PS270-A		0.85	0.98	1.1	9.8
PS660-B	PS740-A		0.31	0.40	0.42	11.3
PS2600-B	PS3300-A		turbid	0.14	0.16	7.8
Benzil	9-methyl- anthra- cene	butan- one	5.1	5.3	5.6	6.6
PS23-B	PS25-A		2.0	2.6	2.7	13.0
PS60-B	PS71-A		1.5	1.6	2.1	13.6
PS210-B	PS270-A		0.87	0.88	1.1	10.7
PS660-B	PS740-A		0.56	0.66	0.89	14.7

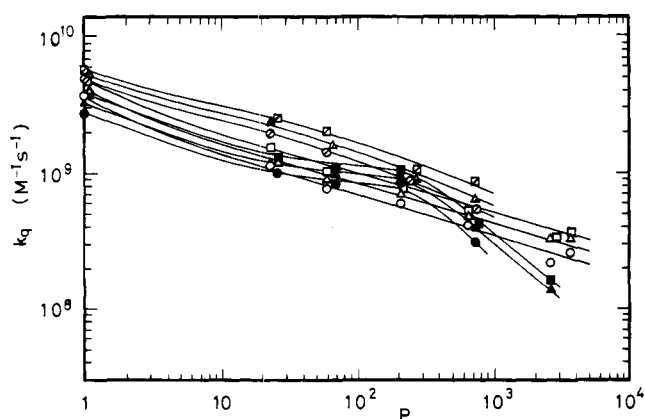


Figure 2. Dependences of k_q on the degree of polymerization P in benzene (\circ , Δ , \square), cyclohexane (\bullet , \blacktriangle , \blacksquare), and butanone (\circ , Δ , \square). Plots for $P = 1$ correspond to the reaction of benzil with 9-methylanthracene. Temperatures: (\circ , \bullet , \circ) 20 °C; (Δ , \blacktriangle , Δ) 30 °C; (\square , \blacksquare , \square) 40 °C.

increasing degree of polymerization. Thus, the rate constant for PS2600-B and PS3300-A in cyclohexane at 20 °C could not be measured since the solution became turbid at that temperature.

The reciprocal triplet lifetimes $1/\tau_0$ of PS-B varied widely according to samples and solvents. This is probably due to impurities which attached to the polymer chains during the preparation as already mentioned.¹ The values of τ_0 for PS-B in cyclohexane were larger than τ_0 of the corresponding PS-B in benzene.

Rate Constants between PS-B and PS-A in Various Solvents

The rate constants k_q for quenching of PS-B by PS-A measured in the present work are summarized in Table III. The magnitude of k_q for polymer–polymer reactions lies in the range of 2×10^9 – $1 \times 10^8 \text{ M}^{-1} \text{ s}^{-1}$ and decreases with increasing degree of polymerization. The activation energies E_q in Table III show some scatter due to the influence of errors in k_q but seem to be independent of the molecular weights of PS-B and PS-A, and are compared with temperature dependences of the solvent viscosities (10.6 kJ/mol for benzene, 11.9 kJ/mol for cyclohexane, 8.4 kJ/mol for butanone).¹²

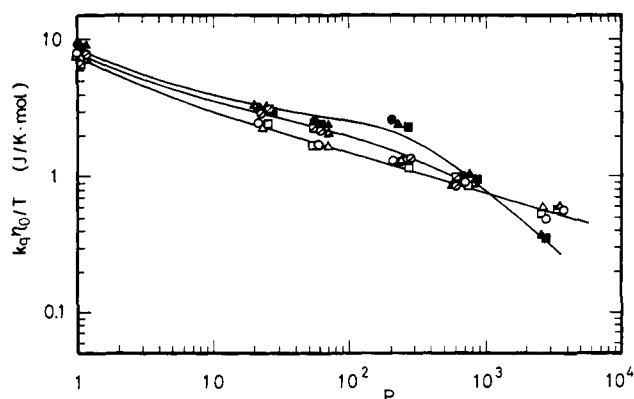


Figure 3. Reduced rate constants $k_q\eta_0/T$ against P for polymer–polymer reactions in various solvents. Symbols are the same as indicated in Figure 2.

Dependences of k_q on degree of polymerization P of PS-B and PS-A are illustrated in Figure 2 including the results obtained in the previous work.¹ Almost straight lines are given for k_q in benzene on log–log graph paper. The slopes show that k_q in benzene is approximately proportional to $P^{-0.29}$ for the range of $P = 23$ –3900. The rate constants k_q in butanone are larger than the corresponding k_q in benzene due to a smaller viscosity of butanone and the change in the interaction parameter. The rate constants k_q in cyclohexane show sigmoidal dependence on P and become smaller than the corresponding k_q in benzene in the case of $P > 2 \times 10^3$.

Translational diffusion coefficient of the polymer molecule composed of n segments D_{pt} and the translational diffusion coefficient of segment $D_s(r)$ at the distance r from the center of mass have been expressed in eq 2¹³ and 3,²

$$D_{pt} = (k_B T / 6\pi n \eta_0 a_m) (1 + 8\lambda_0 n^{1/2} / 3) \quad (2)$$

$$D_s(r) = (k_B T / 6\pi \eta_0 a_m) \times [1 - \{1 - (1 + 8\lambda_0 n^{1/2} / 3) / n\} \exp(-9r^2 / nb^2)] \quad (3)$$

where

$$\lambda_0 = \zeta_0 / 6^{1/2} \pi^{3/2} \eta_0 b \quad (4)$$

and notations are the same as previously described.¹ In order to remove the influences of solvent viscosity, η_0 , and reaction temperature, T , on k_q , k_q can be multiplied by η_0/T by considering eq 2 and 3 regardless of whether the rates are controlled by the translational diffusion step of the polymer molecule or by that of the segment carrying the active group.

The reduced rate constants $k_q\eta_0/T$ are shown in Figure 3 against P . The values of $k_q\eta_0/T$ for different T in each solvent fit in with a single normalized curve characterizing the excluded volume effect in each polymer–solvent system. In the range of $P < 2 \times 10^2$, the poorer the solvent, the larger $k_q\eta_0/T$ becomes for the same degree of polymerization. This tendency is in accord with theoretical models^{2–4,8} proposed by the consideration of equilibrium potential energy between two polymer molecules as a function of distance between their centers of mass. The $k_q\eta_0/T$ in poor solvent especially in cyclohexane decrease markedly with further increase in P and become about a half $k_q\eta_0/T$ in benzene for $P = 3 \times 10^3$. This inversion is supported by the experimental results reported in ref 5–7 and 9 which have been obtained for polymers with $P > 10^3$. The present measurements over the wide range of P have confirmed the inversion of solvent dependence of the reactivity for polymer–polymer reactions according to smaller or larger P regions.

Table IV
Comparison of Calculated Values of $k_q\eta_0/T$ with Experimental Ones for Reactions between PS-B and PS-A in Benzene (BZ), Butanone (BN), and Cyclohexane (CH)

P in PS-B	P in PS-A	n	α^2 ^a			$(k_q\eta_0/T)_{\text{calcd}}, \text{J K}^{-1} \text{mol}^{-1}$			$(k_q\eta_0/T)_{\text{exptl}}, \text{J K}^{-1} \text{mol}^{-1}$		
			BZ	BN	CH (40 °C)	BZ	BN	CH (40 °C)	BZ	BN	CH (40 °C)
23	25	2.3	1.19	1.02	1.01	2.4	2.9	2.9	2.4	3.0	3.0
60	71	6.2	1.27	1.04	1.01	1.8	2.2	2.3	1.7	2.2	2.5
210	270	23	1.41	1.06	1.02	1.3	1.8	1.9	1.3	1.2	2.5
660	740	66	1.58	1.09	1.03	1.1	1.6	1.7	0.87	0.92	0.94
2600	3300	278	1.88	1.17	1.06	0.88	1.4	1.6	0.53		0.35
2900	3900	321	1.91	1.17	1.06	0.87	1.4	1.6	0.59		

^a Calculated from data in benzene,²² butanone,²³ and cyclohexane,¹¹ respectively.

The conflict in literature²⁻⁹ concerning the excluded volume effect on polymer-polymer reactions will be resolved in the following manner.

The excluded volume effect on diffusion-controlled polymer-polymer reactions includes the thermodynamic (equilibrium) aspect and the kinetic (nonequilibrium) aspect. The effect of thermodynamic excluded volume makes the rates in good solvents smaller than rates in poor solvents for polymers of $P < 10^3$, as has been expected by theoretical models.^{2-4,8} However, the appearance of a kinetic excluded volume inverts the results for polymers with a higher degree of polymerization. As the kinetic excluded volume is thought to arise from a topological hindrance of polymer chains for the approach of reacting active sites to each other, its effect would be naturally enhanced by the increase in molecular weight and segment density. This is what Cameron et al.⁵ and Schnabel et al.^{6,7} have described tentatively for the explanation of their experimental results. Detailed discussion will be given in the next section.

Comparison of Results with Theoretical Model

A theoretical model for diffusion-controlled intermolecular reactions has been presented for the first time by the present authors^{2,14} which includes the excluded volume effect of the polymer chain. The model regards the segmental diffusion as a rate-determining step and is composed of a segmental diffusion coefficient depending on the position $D_s(r)$, Smoluchowski equation, and potential energy function for intermolecular interaction.

According to this model, the quenching rate constants k_q can be given by

$$k_q = A(\alpha)B(n)C(\zeta_0, T) \quad (5)$$

$$A(\alpha) = (27/2\pi^{1/2}) \int_0^\infty \exp\{-3^{3/2}z\alpha^{-3} \exp(-9x^2/2)\}x^2 \times \exp(-9x^2/4) dx \quad (6)$$

$$B(n) = (108/\pi^{1/2}) \int_0^\infty [1 - \{1 - (1 + 8\lambda_0 n^{1/2}/3)/n\} \exp(-9y^2)]y^2 \exp(-9y^2) dy \quad (7)$$

$$C(\zeta_0, T) = 4 \times 10^{-3} R_s N_A k_B T / 3 N_0 \eta_0 a_m \quad (\text{in } \text{M}^{-1} \text{s}^{-1}) \quad (8)$$

where all notations are the same as originally given² and an erratum in numerical coefficient in original eq 45 is corrected. For the reduced rate constant $k_q\eta_0/T$, eq 5 and 8 are transformed to

$$k_q\eta_0/T = A(\alpha)B(n)C_0 \quad (9)$$

$$C_0 = 4 R_s N_A k_B / 3 N_0 a_m \quad (\text{in } \text{J K}^{-1} \text{mol}^{-1}) \quad (10)$$

where k_B should be given in J/K. The effective radius of triplet-triplet energy transfer R_s is supposed to be 13.7 \AA ¹⁵ multiplied by 0.61¹ as a steric hindrance factor due to the introduction of the alkyl group at 9 position of anthracene.

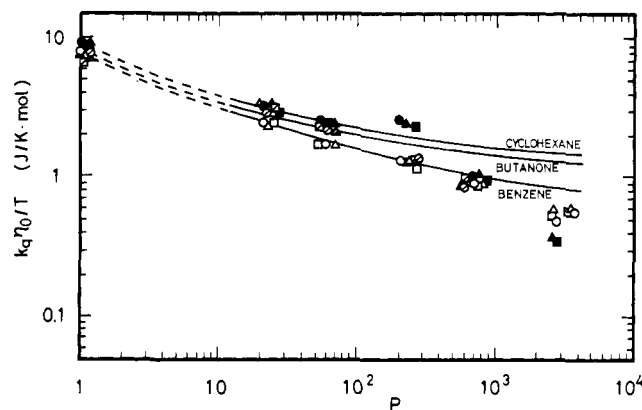


Figure 4. Comparison of calculated $k_q\eta_0/T$ (solid lines) with experimental $k_q\eta_0/T$ in benzene (O, Δ , \square), cyclohexane (\bullet , \blacktriangle , \blacksquare), and butanone (\circ , \triangle , \square).

The number of monomer units in a segment N_0 and the hydrodynamic radius of monomer unit a_m are supposed to be 10.6^{16} and 3.65 \AA ,¹⁷ respectively, for the present system according to their definitions in the model.

The calculated and experimentally found values of $k_q\eta_0/T$ are listed in Table IV together with the number of segments n and expansion factor α^2 used for the calculation. The values of n , α^2 , and $k_q\eta_0/T$ are averaged ones for both components in each system. The coincidence of $(k_q\eta_0/T)_{\text{calcd}}$ with $(k_q\eta_0/T)_{\text{exptl}}$ in cases of comparatively low degree of polymerization is rather striking in view of the fact that eq 6, 7, 9, and 10 contain no arbitrarily adjustable parameters. In cases of higher degree of polymerization, the experimental values of $k_q\eta_0/T$ in benzene fall a little compared with the supposed values by the model, and the deviation becomes more marked in poor solvents. This will be noticed more clearly in Figure 4, where curves for calculated values of $k_q\eta_0/T$ against P are compared with experimental results.

In the model used here for the calculation, the effect of excluded volume has been introduced by the use of expansion factor α and potential energy of interaction $\Delta F(a)$ between two molecules in the distance a . In other words, only the thermodynamic aspect of the excluded volume has been considered in the model. The agreement of $(k_q\eta_0/T)_{\text{exptl}}$ with $(k_q\eta_0/T)_{\text{calcd}}$ for $P < 10^3$ in benzene and for $P < 10^2$ in butanone and cyclohexane suggests that the real (not time averaged) conformation of the polymer chain for these cases is not like a sphere coil but like a reptile and the polymer chain does not occlude its end group during the reaction. Residual polymer chains in these cases affect the reaction rates between chain end groups through their influence on segmental diffusion coefficient and spatial distribution of chain end segments.

In cases of $P > 10^3$ especially in poor solvent, the polymer chain gives an additional kinetic effect on the

reaction rates. This effect represents the phenomenon that chain end A, on its way to reacting with chain end B, bumps into other portions of polymer chains of PS-A or PS-B and thus has its progress toward reaction retarded. This kinetic excluded volume effect should be distinguished from the thermodynamic one, since a thermodynamically stable overlapped state, even if it exists, cannot be attained at once due to the topological hindrance of polymer chains against interpenetration. The concept of kinetic excluded volume effect on reactions given here has been first presented by Wetmur¹⁸ for the rates of renaturation of DNA. Morawetz et al.^{8,9} have also discussed the kinetic excluded volume effect, but their theoretical model was not concerned with the kinetic excluded volume effect but with the thermodynamic one in the present meaning.

The influence of segment density on the reaction rates is one of the important points used to distinguish the kinetic excluded volume effect from the thermodynamic one. In contrast to the fact that the thermodynamically excluded volume decreases in poorer solvents corresponding to higher segment density, the effect of polymer chains as the topological barrier for the reaction is supposed to increase with increasing segment density around the active sites. This tendency will be enhanced by the increase in degree of polymerization and/or in poor solvent, since the reacting active sites have to pass through a larger number of segments in these cases. The segment density within 100 Å from the chain end group in cyclohexane was calculated to be about twice as large as that in benzene for $P = 3 \times 10^3$. This corresponds to the fact that $k_q\eta_0/T$ in cyclohexane is about a half $k_q\eta_0/T$ in benzene for the cases of PS2600-B and PS3300-A. The same tendency has already been suggested tentatively as to results in literatures.⁵⁻⁷

The kinetic excluded volume effect would be associated with the rate of interpenetration between polymer molecules. Yasukawa et al.¹⁹ have shown by Monte-Carlo technique the character of topological hindrance of polymer chains for the encounter of chain ends. Wetmur¹⁸ has introduced in his kinetic model an assumption that two polymers can overlap only to the distance where the probability that any segments from the two polymers occupy the same volume element is less than unity. Thus he tried to relate the kinetic excluded volume effect to the degree of interpenetration. The degree of interpenetration, however, is thought to be of thermodynamic character which can be measured by equilibrium experiments and discussed by the use of pair potential. For example, Worsford²⁰ has indicated the possibility of complete interpenetration in concentrated polymer solution in good solvent, but a very long time was required to attain the equilibrium fully interpenetrating state in the concentrated solution. Moreover, the degree of interpenetration has been reduced to 0.6–0.7 in dilute solution. Olaj et al.²¹ have calculated by the Monte-Carlo technique the pair potential $U(a)$ between two polymers as a function of the distance a between centers of mass in the Θ conditions and shown the existence of a repulsive potential even in the Θ con-

ditions. Their technique includes the effect of segment density on the pair potential but is not concerned with the topological hindrance between polymer chains during the course of interpenetration of two initially isolated molecules. Thus, the examination of the parallelism between the degree of interpenetration and the rate of interpenetration is required for further investigation but is supposed to be beyond the scope of the present paper. So it is difficult so far to give a quantitative discussion on the effect of kinetic excluded volume. Nevertheless, the present results reveal the importance of the kinetic excluded volume effect as well as the thermodynamic one on polymer–polymer reactions.

In conclusion, the measurements of diffusion-controlled rates between chain end groups attached to different monodisperse flexible polymers by the triplet probe method have shown that reduced rate constants $k_q\eta_0/T$ in poor solvents are larger for $P < 10^3$ and smaller for $P > 10^3$ than $k_q\eta_0/T$ in good solvent. The results for lower P have been explained well by the previously proposed model² including the thermodynamic excluded volume effect, whereas the results for higher P require the concept of the kinetic excluded volume effect.

Acknowledgment. The authors express their gratitude to Associate Professor T. Fukutomi of Tokyo Institute of Technology for his kind discussions. The present work was supported by the Grant for Scientific Researches from the Ministry of Education, Japan.

References and Notes

- (1) K. Horie and I. Mita, *Polym. J.*, **9**, 201 (1977).
- (2) K. Horie, I. Mita, and H. Kambe, *Polym. J.*, **4**, 341 (1973).
- (3) K. Ito, *J. Polym. Sci., Polym. Chem. Ed.*, **10**, 3159 (1972).
- (4) H. K. Mahabadi and K. F. O'Driscoll, *J. Polym. Sci., Polym. Chem. Ed.*, **15**, 283 (1977).
- (5) G. G. Cameron and J. Cameron, *Polymer*, **14**, 107 (1973).
- (6) W. Görlich and W. Schnabel, *Makromol. Chem.*, **164**, 225 (1973).
- (7) J. Kiwi and W. Schnabel, *Macromolecules*, **9**, 468 (1976).
- (8) H. Morawetz, J. R. Cho, and P. J. Gans, *Macromolecules*, **6**, 624 (1973).
- (9) J. R. Cho and H. Morawetz, *Macromolecules*, **6**, 628 (1973).
- (10) J. P. Cotton, B. Farnoux, and G. Jannink, *J. Chem. Phys.*, **57**, 290 (1972).
- (11) W. R. Krigbaum and D. K. Carpenter, *J. Phys. Chem.*, **59**, 1166 (1955).
- (12) Chemical Society of Japan, "Kagaku Binran, Kiso-hen II", Maruzen, Tokyo, 1975, p 575.
- (13) J. G. Kirkwood and J. Riseman, *J. Am. Chem. Soc.*, **16**, 565 (1948).
- (14) K. Horie, I. Mita, and H. Kambe, paper presented at the 21st meeting of the Polymer Society of Japan, Tokyo, 1972.
- (15) H. Kobashi, T. Morita, and N. Mataga, *Chem. Phys. Lett.*, **20**, 376 (1973).
- (16) W. R. Krigbaum, J. E. Kurz, and P. Smith, *J. Phys. Chem.*, **65**, 1984 (1961).
- (17) J. T. Edward, *J. Chem. Educ.*, **47**, 261 (1970).
- (18) J. G. Wetmur, *Biopolymers*, **10**, 601 (1971).
- (19) T. Yasukawa and K. Murakami, *Makromol. Chem.*, **175**, 2769 (1974).
- (20) D. J. Worsford, *J. Polym. Sci., Polym. Chem. Ed.*, **12**, 337 (1974).
- (21) O. F. Olaj and K. H. Pelinka, *Makromol. Chem.*, **177**, 3413 (1976).
- (22) T. Altares, Jr., D. P. Wyman, and V. R. Allen, *J. Polym. Sci., Part A*, **2**, 4533 (1964).
- (23) P. Outer, C. I. Carr, and B. H. Zimm, *J. Chem. Phys.*, **18**, 830 (1950).